

# CFD Investigation on the Application of Optimum Non-Axisymmetric Endwall Profiling for a Vaned Diffuse

L. Zhou<sup>†</sup>, F. Xiang and Z. Wang

*Shaanxi Key Laboratory of Internal Aerodynamics in Aero-Engine, School of Power and Energy, Northwestern Polytechnical University, Xi'an, Shan Xi Province, 710072, China*

<sup>†</sup>Corresponding Author Email: [zhouli@nwpu.edu.cn](mailto:zhouli@nwpu.edu.cn)

(Received December 5, 2017; accepted June 25, 2018)

## ABSTRACT

In order to improve the performance of a transonic centrifugal compressor stage, non-axisymmetric endwall profiling optimization was conducted for the diffuser under design condition, Artificial Neural Network (ANN) and Genetic Algorithm (GA) were used to execute the optimization with the objective of maximizing the isentropic efficiency of the compressor stage. The influence mechanism of non-axisymmetric endwall profiling on flow field and performance was discussed. Results show non-axisymmetric endwall profiling is an effective way to significantly reduce the flow loss in the diffuser. The total pressure loss of the diffuser decreases by 9.31% and 20.29% for NA0.70 and NA1.40 respectively. The profiled endwall suppresses the flow separation through accelerating the low-energy flow and reducing lateral pressure gradient. The corresponding high vorticity within the flow separation zone is reduced, which delays the formation and development of the flow separation. The diffuser becomes more fore-loaded, the overall blade loading is not affected, and the pressure ratio of the compressor stage is improved as well. At the outlet of the diffuser, the more uniform flow angle and much lower total pressure loss along spanwise are obtained. However, the backflow with high velocity gathering near the shroud of the diffuser makes the mass flow rate decrease and easily induce the stall, which results in the smaller operating range for both profiled endwall.

**Keywords:** Diffuser; Non-axisymmetric endwall profiling; Optimization design; Total pressure loss; Flow separation.

## NOMENCLATURE

CLC	total pressure loss coefficient of diffuser	TE	trailing edge
Cr	radial chord	$V_r$	radial velocity
H	vane height	$y^+$	non-dimensional wall distance
LE	leading edge	$\Delta$	change in property
M	mass flow	$\eta$	isentropic stage efficiency

## 1. INTRODUCTION

With the advantage of compact structure, high pressure ratio of the single stage and widely stable operating range, centrifugal compressor has been massively applied in the small gas turbine engines (Wang *et al.* 2011). Researches have shown that the flow loss in the diffuser accounts for about 30% of the total loss in the centrifugal compressor, and the diffuser has an important effect on efficiency, pressure ratio and operating range of the centrifugal compressor stage (Ferrara *et al.* 2002 a b), but it is difficult to achieve high-efficiency due to the

restriction of the flow separation, which happens frequently in the diffuser passage (Gao *et al.* 2005). In order to improve the performance of the diffuser, the boundary layer thickness must be effectively controlled to reduce the separation loss as much as possible. The popular methods currently used for reducing the flow loss include low solidity diffuser (Mukkavilli *et al.* 2002), adjustable vane (Xi *et al.* 2006), tandem cascade (Zhao and Wang 1997) and boundary layer suction technique (Zhao *et al.* 2009) *et al.*, mainly concentrating on the shape modification of the diffuser vane. However, these methods induce the extra complexity of the vane

configuration, which could be a challenge for the diffuser design and manufacture.

As a passive flow control approach, non-axisymmetric endwall profiling can effectively suppress the secondary flow and flow separation, in which concave-convexity profiling is applied on the endwall to reduce the lateral pressure difference. This technology is based on the principle that convexity curvature of the wall can locally accelerate flow and reduce the local static pressure, while concave curvature causes a relative diffusion, which increases the local static pressure (Chu *et al.* 2016). As early as 1975, Morris (1975) had proposed concept of the endwall profiling to decrease the flow loss. The profiled endwall was first successfully applied for the turbine stator by Rose (1994), the non-uniformity of the lateral pressure distribution was declined by 70%. Hoeger *et al.* (2002) studied the transonic compressor rotor with endwall profiling, a total pressure loss reduction by 30% and efficiency improvement of 0.5% were achieved. Harvey (2008 a, b) carried out experimental research on the linear stator cascade of the compressor, results showed that the non-axisymmetric endwall could effectively suppress the secondary flow in the cascade passage, then reduced the flow loss. Nagel *et al.* (2005) presented a revolutionary integrated design which optimized both the blade modeling and endwall profiling. Moreover, measurements indicated that satisfactory performance had been achieved for the designed turbine. Since then, this approach gradually attracted researchers' attentions to pursue the higher performance potential (Pochler *et al.* 2015 a, b; Li *et al.* 2005) proposed an endwall profiling method based on trigonometric function, and the secondary flow was significantly weakened after endwall profiling was applied in a transonic cascade, leading to a reduction by 4.7% of total pressure loss. Liu *et al.* (2008) discussed the flow mechanism of non-axisymmetric endwall through numerical simulations of the turbine cascade with different endwall profilings. In the numerical optimization of a high load compressor cascade conducted by Wu (2011), the total pressure loss was obviously decreased, the corresponding secondary flow loss was minimum when the concave-convexity amplitude was 4% of blade height. Since the non-axisymmetric endwall design using the optimization algorithm is effective to reduce the flow loss, the non-axisymmetric endwall profiling had been widely adopted (Zhang *et al.* 2014; Guo *et al.* 2016).

With the development of the centrifugal compressor toward to high load and wide operating condition range, and flow separation definitely occurs in the diffuser with the traditional single cascade adopted for the vaned diffuser. Higher demands is put forward to the ability of the diffuser, which not only increase of the flow turning angle, but also effective control of the flow loss under different operating conditions. Thus, it is necessary to discuss different kinds of flow control techniques, obtaining an appropriate way to reduce the flow loss in the diffuser. The above studies show that the non-

axisymmetric endwall profiling has an impressive potential to reduce the flow loss in the turbine and the axial compressor cascades. Therefore, it's worth exploring the application of endwall profiling in the diffuser for the flow loss control near the endwall of diffuser. In this paper, non-axisymmetric endwall profiling and optimization was employed in the diffuser, and then to compare with the tandem cascade vane diffuser, to confirm the efficient approach to improve the performance of centrifugal compressor.

## 2. NUMERICAL SIMULATION METHODOLOGY

A single stage centrifugal compressor was investigated numerically in this paper using NUMECA Fine/Turbo. 3D steady Reynolds averaged Navier-Stokes equations was solved with Spalart-Allmaras turbulence model adopted. Equations were discretized in the finite volume form on each of the hexahedral control volume with cell center variable storage, center difference scheme was used in the spatial discretization with second-order accuracy in space. The basic algorithm is a four-step Runge-Kutta method. In order to reduce the computation cost, the discretized equations are solved using accelerating techniques, such as local-time stepping, multigrid method and implicit residual smoothing.

The fore-loaded airfoil diffuser with aspect ratio of 4.44 was presented in Fig. 1. In order to obtain the true inlet boundary condition of the diffuser, the calculation was performed for the compressor stage, with the calculation domain including one impeller passage and one diffuser passage, and Table 1 shows main geometric parameters of the centrifugal compressor. The structured grids were generated with refinement near walls to ensure that  $y^+ < 10$ , as shown in Fig. 2. To evaluate the effect of mesh size on the numerical results, three mesh are adopted, which are 0.45 million, 0.94 million and 1.8 million respectively. Static pressure distributions on 50% span of the diffuser vane are compared in Fig. 3. The result of grid independence check shows the maximum error is 1.3%, and the relative error at most of the positions is smaller than 1% when the mesh number is larger than 0.94 million. Thus, the mesh number with 0.94 million is used for flow analysis in the paper. In the calculation, pressure-inlet boundary condition was specified at the impeller inlet, flow angle (axial inflow), total pressure and total temperature were imposed, and pressure-outlet boundary condition was set at the diffuser outlet, static pressure was imposed and other variables were extrapolated from the interior. No-slip and adiabatic wall boundaries were applied on the solid wall. Periodic boundary condition were adopted at the circumferential boundary. The mixing plane was adopted on the impeller / diffuser interface to transfer flow information between two rows.

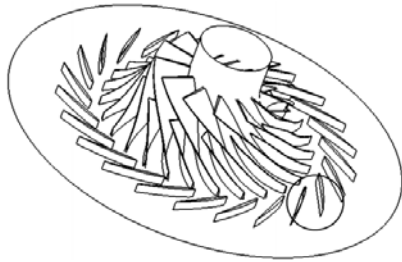


Fig. 1. Centrifugal compressor model

Table 1 Main geometric parameters of the centrifugal compressor

parameters	value
main / splitter blade number	13/13
impeller outlet radius $R_2$ (mm)	81
diffuser vane number	23
diffuser inlet radius $R_3$ (mm)	89
diffuser outlet radius $R_4$ (mm)	114
diffuser vane height $H$ (mm)	7.024
diffuser aspect ratio	4.44

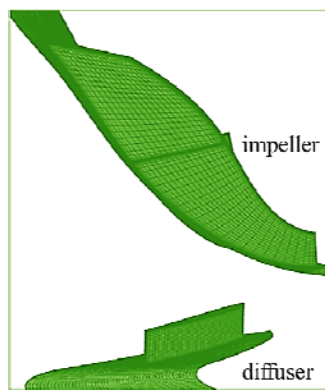


Fig. 2. Computational grid

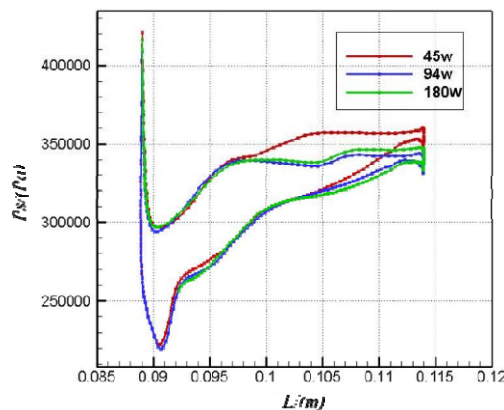


Fig. 3. Static pressure distributions under different mesh size

In order to get the suitable approach of reducing flow loss in the diffuser, the non-axisymmetric endwall profiling optimization is carried out for the hub region of the diffuser. In addition, the tandem cascade diffuser was designed and compared with

the non-axisymmetric endwall to estimate their capacities for improving the centrifugal compressor performance.

### 3. NON-AXISYMMETRIC ENDWALL OPTIMIZATION

#### 3.1 Endwall Parametrization

Parametric modeling is performed for the diffuser for preparing the non-axisymmetric endwall optimization. After the initial diffuser vane and endwall are fitted, geometric structures that can be controlled by parameters are generated to provide subsequent optimization variables. The flow passage enclosed by one concave surface and the adjacent convexity surface of the diffuser vane is selected as the modeling region. The parameterized hub in this paper starts at the leading edge and ends at the trailing edge of the diffuser vane. As shown in Figs. 4, 5 cutting lines are selected along the circumferential direction, 2 camber lines of adjacent vanes, together with 3 cutting lines paralleling to the camber line, evenly divide the endwall into four parts. With 5 control points uniformly distributed along each cutting line, the parametrization produces 25 free control points in total. Once the coordinates of these points are defined, the endwall control line can be generated by using the Bezier curve, and the non-axisymmetric endwall can be flexibly adjusted by these 25 control points, forming different non-axisymmetric structure.

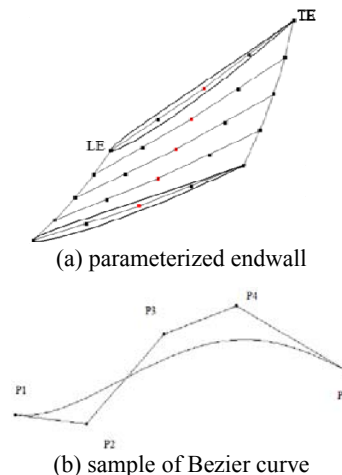


Fig. 4. Endwall parameterization sketch

#### 3.2 Endwall Optimization

Demeulenaere *et al.* (2005) presented an integrated environment NUMECA /Design3D developed for the optimization of turbomachinery blade shapes, and significant improvements were obtained in terms of efficiency and pressure rise. NUMECA/Design3D which has been considered as a useful optimization tool is chosen to perform the endwall optimization in this paper. Axial coordinates of above 25 control points are selected as the optimization variables. The optimization procedure is depicted in Fig. 5, the initial sample database is generated randomly under the constraint of these independent variables. The Artificial

Neural Network (ANN) has been adopted to establish the approximate function between the sample calculation results and optimization variables. On the basis of the approximation function model, the optimum geometry is searched by Genetic Algorithm (GA), and then validated by CFD approach, the optimization can be completed if the objective function is satisfied. Otherwise, the calculation result of the current iteration is added into the database as a new sample, then enters in the next iteration until the optimization target is met finally. Furthermore, ANN and GA are combined in the optimization process, which can save the computation cost and accelerate the convergence.

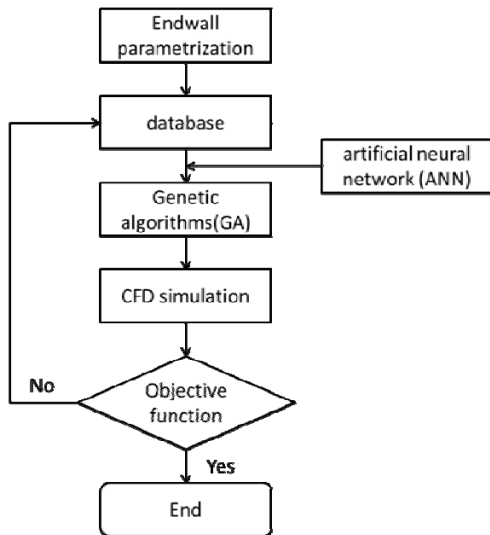
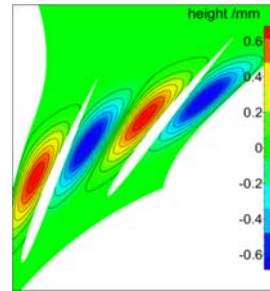


Fig. 5. Flow chart of optimization system

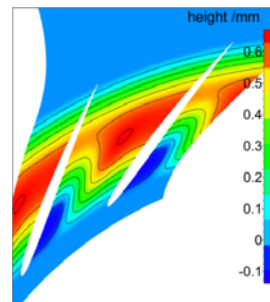
Two different initial databases are tested, with 80 samples involved for each case. The axial variation range of control points of these two databases are restricted to  $\pm 0.70\text{mm}$  (10% H) and  $\pm 1.40\text{mm}$  (20% H) respectively, which are divided into 4 regions according to the discrete sampling method. The optimization objective is set to maximize the isentropic efficiency of the compressor stage under the design condition.

The optimum endwalls are named as NA0.70 and NA1.40 according to their variation range of the control points. As a reference group, the conventionally non-axisymmetric endwall profiling named as NATrad is adopted without optimization, whose endwall profiling is downward concave on the suction side and upward convexity on the pressure side, and the concave-convexity amplitude of NATrad is same with that of NA0.70. Figure 6 shows the height distribution of the non-axisymmetric endwall profiling, both the concave amplitude and convexity amplitude are 0.67mm (9.5% H) for NATrad, and uniformly distributes along the circumferential direction. Non-uniform height distribution appears in other two optimized endwall profiling, remaining the same concave-convexity trend except for the magnitude. These two optimized endwalls are mainly characterized by convexity on the whole pressure side and rear part of the suction side, while a small local concave is formed in the front part of suction side. The convexity amplitudes of NA0.70 are

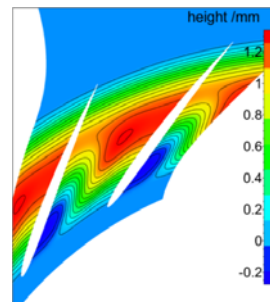
0.66mm on pressure side and 0.56mm on rear part of the suction side, which are 9.4%H and 8%H respectively, and the concave amplitude is 0.14mm (2% H) in the front part of suction side. Figure 6d shows sketches of the diffusers with and without endwall profiling, it clearly shows the concave-convexity amplitude of the endwall increase when the endwall profiling is adopted, and the maximum concave-convexity amplitude obviously increases from NA 0.7 to NA1.40. For the non-axisymmetric endwall of NA1.40, the maximum concave-convexity amplitude increases up to 18.5% H on pressure side, 15.7% H on rear part of the suction side, and 3.6% H on the front part of suction side.



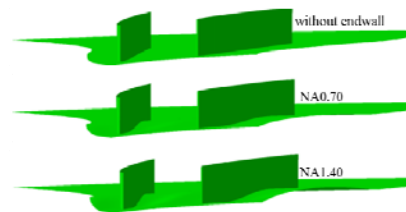
(a)NATrad



(b)NA0.70



(c)NA1.40



(d) sketches of the diffusers

Fig. 6. Height distribution of non-axisymmetric endwall

#### 4. RESULTS AND DISCUSSION

##### 4.1 Aerodynamic Performance

The total pressure loss coefficient of the diffuser is defined as follow:

$$C_{LC} = \frac{P_{t3} - P_{t4}}{P_{t3} - P_3} \quad (5)$$

Where  $P_{t3}$  and  $P_{t4}$  is the total pressure at diffuser inlet and diffuser outlet respectively.  $P_3$  represents the static pressure at diffuser inlet (Zhang *et al.* 2009).

The isentropic efficiency of centrifugal compressor stage and total pressure loss coefficient of the diffuser are listed in Table 2 with different endwall profilings and the tandem cascade diffuser. It can be seen that two optimized non-axisymmetric endwalls turn out to attain a significant efficiency improvement than the baseline diffuser, but the reference group NAtrad has a slightly adverse effect on performance. The isentropic efficiency of NA0.70 increases by 1.68%, and the total pressure loss of the diffuser decreases by 9.31%. The efficiency of NA1.40 rises by 3.63%, the reduction of its total pressure loss reaches impressively 20.29%. On the contrary, efficiency of the non-optimized endwall of NAtrad is reduced by 0.12%, the total pressure loss is increased by 0.57% as well. When the tandem cascade diffuser is adopted for the compressor stage, the efficiency increases by 2.46% and total pressure loss reduces by 13.30%. The ability of tandem cascade diffuser to improve the compressor performance under design condition is between optimized non-axisymmetric endwall profiling of NA0.70 and NA1.40.

**Table 2 Performance parameters under design condition**

	$\eta$	$\Delta\eta$ (%)	$C_{LC}$	$\Delta C_{LC}$ (%)
baseline	0.7609	0	0.4047	0
NAtrad	0.76	-0.12	0.4070	0.57
NA0.70	0.7737	1.68	0.3671	-9.31
NA1.40	0.7885	3.63	0.3226	-20.29
tandem	0.7796	2.46	0.3509	-13.30

The performance map of the centrifugal compressor stage under different diffuser configuration are displayed in Fig. 7. When the compressor is operated close to the stall boundary, the efficiency improvement effectiveness of the profiled endwall keeps the same level as the case under design condition. The efficiency benefit of NA0.70 and NA1.40 are 1.51% and 3.21% severally. The positive impact of non-axisymmetric endwall near the blockage boundary are even better than that it has under the design condition, efficiency of

NA0.70 and NA1.40 increases by 2.64%, 3.97% respectively.

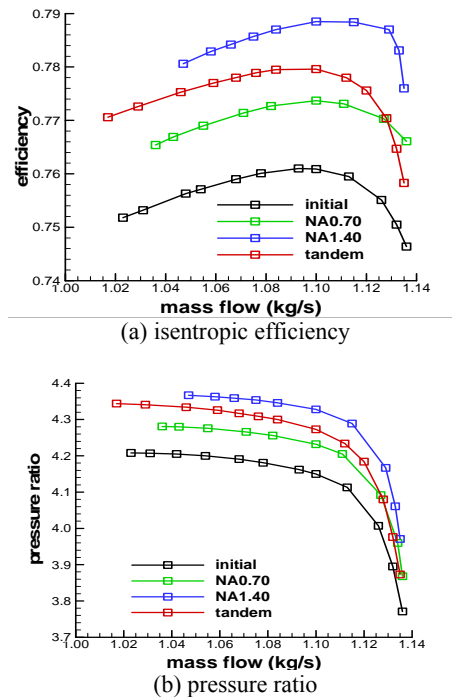


**Fig. 7. Performance map under different diffuser configuration**

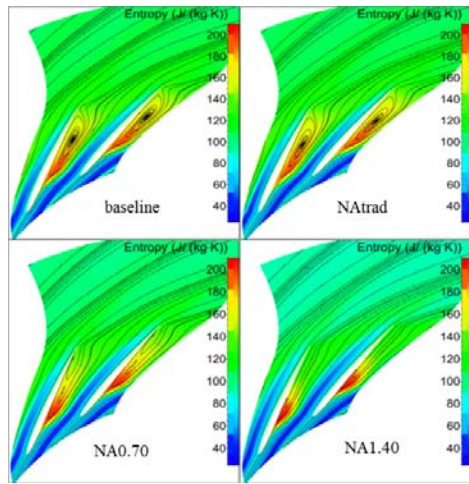
In the whole operation range, notable improvement of efficiency and pressure ratio confirm the potential of the non-axisymmetric endwall profiling. However, a smaller stable operating range couldn't be ignored, the operating range of NA0.70 decreases by 11.50%, and the reduction achieves to 22.12% for NA1.40. The main reason is that the upward convexity covers most part of endwall, resulting in the reduction of the effective flow area in the diffuser passage. Similarly, when the tandem cascade diffuser is adopted, the efficiency and pressure ratio are both improved evidently. The phenomenon of the reduction of the operation range is not occurred. At the same time, the flow range of compressor with tandem cascade diffuser increases by 4.42%.

The effect of non-axisymmetric endwall at larger mass flow is better than the smaller flow rate conditions, while the tandem cascade diffuser shows an opposite trend, its performance improvement under the small flow rate condition is more significant. It also can be found that tandem cascade diffuser is an effective way to improve the performance of centrifugal compressor, but its effect is between two kinds of optimized non-axisymmetric endwall. From the comparison, it denotes that optimized non-axisymmetric endwall profiling for the diffuser can notably improve the performance of the centrifugal compressor, it can be used for performance improvement of the high load centrifugal compressor.

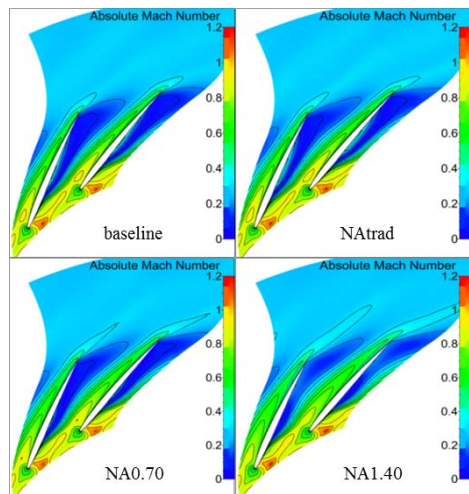
##### 4.2 Flow Field Under Design Condition

Figure 8 presents the flow field at 70% span of the

diffuser. For the baseline diffuser, flow separation occurs near suction side, which corresponds to the region with low Mach number. In this zone, the accumulation of low-energy fluid causes flow loss to rise rapidly, especially at the flow separation origin. When the non-axisymmetric endwall profiling is applied and optimized, the flow separation can be suppressed, the region with high entropy becomes smaller on the suction side, and the flow separation suppression is more effective for the case of NA1.40. According to the height distribution of non-axisymmetric endwall, the convexity surface near suction side forms a convergent channel, which accelerates the flow in the flow separation zone, leading to the restrained separation and smaller flow loss. For the reference group of NAtrad without optimization, it is helpless for the flow near the suction side and endwall corner because of the downward concave surface, the flow with low Mach number massively concentrates at the downward concave of the suction side, the high flow loss remains due to the large size of the flow separation. Therefore, the optimization is essential to the non-axisymmetric endwall profiling in order to achieve the purpose of improving the flow in the diffuser.



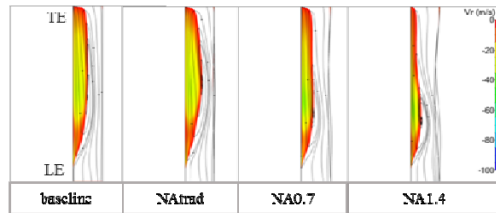
(a) streamline



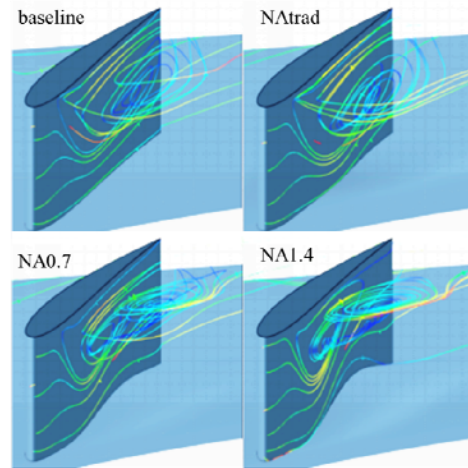
(b) Mach number

**Fig. 8. Flow field at 70% span of the diffuser with different endwall profiling**

The limit streamline with the radial velocity contouring background on suction side and three-dimensional streamline distribution in the diffuser passage are shown in Fig. 9. The area with negative velocity reveals the backflow clearly. Under design condition, the obvious corner separation occupies nearly half of the baseline diffuser passage, which restricts the performance of compressor severely. The coverage of the corner separation apparently becomes smaller at the case of NA0.70 and NA1.40, but the range of the flow separation is enlarged for NAtrad instead. The upward convexity near suction side of the optimized endwall accelerates the low-energy fluid inside the separated vortex, making the separation zone greatly reduced.



(a) limit streamline with Vr contour on suction surface



(b) streamline in the diffuser passage

**Fig. 9. Streamline distribution in the diffuser**

As the hub profiling is performed in the non-axisymmetric endwall optimization process, the corner separation does not occur near the hub, and the smaller flow separation zone moves towards the shroud, hence the negative impact of the flow separation on flow field reduces as compared with the baseline diffuser. In the reference group, the uniformly downward concave surface in the vicinity of the suction side brings a predictable slowdown for the low-speed airflow, the reinforced separation results in the worse performance of the diffuser inevitably.

Figure 10 displays the total pressure loss coefficient distribution on the diffuser vane. When non-axisymmetric endwall profiling is optimized, the total pressure loss is considerably reduced at the rear part of the vane. The loss on pressure side is also dramatically lower than the baseline diffuser at the front part of the vane, while it is nearly unaffected by the endwall profiling on the suction

side. According to the flow characteristics in the diffuser passage, this phenomenon is determined by the local supersonic region which occurs near the leading edge of the suction surface. In order to maintain the curvature continuity of the endwall at the diffuser inlet, the height deviation is relatively small during the endwall profiling process, thus, it is hard to form the complex endwall shape to control the total pressure loss of the transonic flow. On the pressure side, the whole subsonic flow is relatively easier to be controlled by the endwall profiling, and then the flow loss can be reduced obviously. In the reference group of NAtRad, the total pressure loss on both sides of diffuser vane change slightly as compared with the baseline diffuser.

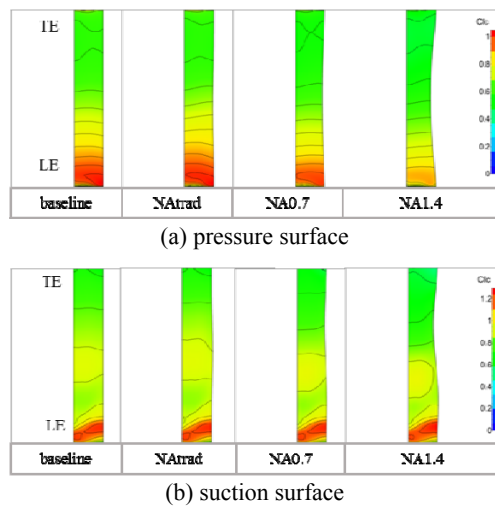


**Fig. 10. Total pressure loss coefficient distribution on the diffuser vane**

The purpose of traditional endwall profiling is to depress the secondary flow through decreasing the transverse pressure gradient between two vanes. Thus the endwall profiling is commonly downward concave on the suction side to increase the local pressure, and upward convexity on the pressure side to decrease the local pressure, then the flow field is improved due to the depression of the secondary flow, which is dominated by the reduction of the transverse pressure gradient. However, the serious corner separation is occurred at the suction side of the baseline diffuser, inducing larger loss and the worse performance. The traditional endwall profiling cannot suppress the flow separation due to the dominated large size of the corner separation, on the contrary, the non-optimized endwall of NAtRad contributes to the extra flow separation, resulting in higher flow loss, thus, the flow field with non-optimized endwall profiling of NAtRad is no longer investigated further in the following sections.

The vorticity distribution at different radial position are presented in Fig. 11, and the development process of vortices can be distinguished. For baseline diffuser, the high vorticity zone begins to concentrate to the midspan of the suction side at 30% Cr (radial chord), and this region corresponds to the large size flow separation, which covers nearly 1/2 of the diffuser passage area.

Subsequently, the flow separation zone is divided into two branches with high vorticity, driven by the interaction between the separated vortex and the low-energy fluid near the endwall. In the downstream passage, the vortex near the shroud keeps growing stronger due to the continuous entrainment of the low-energy flow, and gradually migrates towards the pressure side. Meanwhile, the size and intensity of separated vortex on the suction side are weakened. When the flow arrives at the trailing edge of the diffuser, two small corner separations are formed on both sides of the vane near the shroud. Similar vorticity distribution characteristics are showed for two kinds of optimized non-axisymmetric endwalls at all sections, but the area with high-vorticity and its peak value are reduced evidently as compared with the baseline diffuser. The flow field of the diffuser is improved with the optimized endwall profiling adopted, and the endwall of NA1.40 with larger concave-convexity magnitude is more effective to suppress the secondary flow.

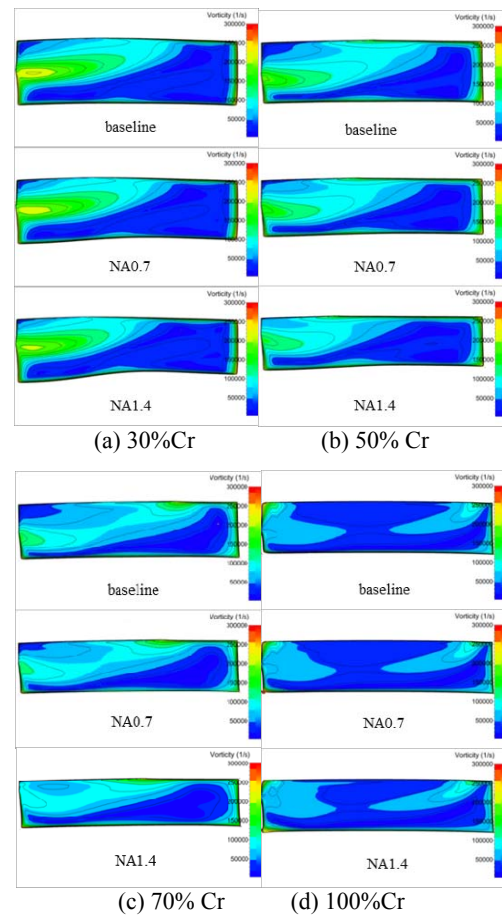


**Fig. 11. Vorticity distribution at different sections in the diffuser**

During the emergence and development process of the flow separation near the suction side, the size and intensity of the separation vortex are decreased owing to the flow adjustment action by the profiled endwall. At the same time, the accumulation of the vorticity near the shroud is delayed, retarding the generation and propagation of the separation vortex. At the trailing edge of the diffuser vane, as shown

in Fig. 11d, the vorticity distributions remain consistent for these three diffusers with different endwall profiling, two accumulation zones are formed near the corner between the diffuser vane and the shroud. However, the corresponding high-vorticity area is apparently smaller with non-axisymmetric endwall adopted, the flow can go through the diffuser passage smoothly.

Static pressure distribution of the vane at different span are displayed in Fig. 12. It shows that the flow field at different span is influenced by non-axisymmetric endwall in the diffuser. The static pressure on the vane decreases firstly and then increases along the streamwise direction for these three spans, which is consistent with the Mach number distribution in Fig. 8. For the baseline diffuser, due to the local supersonic region appeared near the leading edge of the suction side, the pressure fluctuation is relatively large. At 5% span, non-axisymmetric endwall profiling induces a remarkable pressure raise after 30%Cr of the suction side and on the entire pressure side, obvious fore-loaded phenomenon occurs near the hub of the vane. From the Figs. 12b and 12c, it can be seen that the blade loading presents similar variation tendency, the pressure distribution on the suction side is more complex than the simple pressure rise on the pressure side as well. In comparison to the baseline diffuser, the static pressure on the suction side at 50% span and 95% span drops from 10%Cr to 30%Cr, and then increases sharply after 30% Cr.

The pressure distributions on these three spans indicate the following characteristics: a typical fore-loaded property comes into being with the profiled endwall adopted, i.e. blade loading increases at the front part and decreases at the rear part. The local supersonic region on the suction side is not affected by the profiled endwall, due to the failure in formation of non-axisymmetric shape near the diffuser inlet, which is the result of geometric continuity constraint of the endwall profiling.

Based on above features, the majority of the flow separation concentrates in the rear part of the diffuser passage, and the flow field in this region deteriorates seriously. When the non-axisymmetric endwall is adopted, the lateral pressure gradient is reduced in that region, which inhibits the further development of the flow separation. And in the front part of the diffuser passage, the flow is always relatively smooth, the increase of the blade loading can not only ensure the sufficient overall aerodynamic load, but also not induce the additional loss. This is an important reason for non-axisymmetric endwall profiling to improve the compressor efficiency and the pressure ratio simultaneously.

The above analysis shows that a large scale of the flow separation appears on the suction side of the diffuser vane, and with the vortex core located at 50% Cr. The distribution of the total pressure loss coefficient along the spanwise direction is shown in Fig. 13 at the diffuser outlet. The pitchwise averaged total pressure loss coefficient indicates that the flow loss near the shroud is much higher

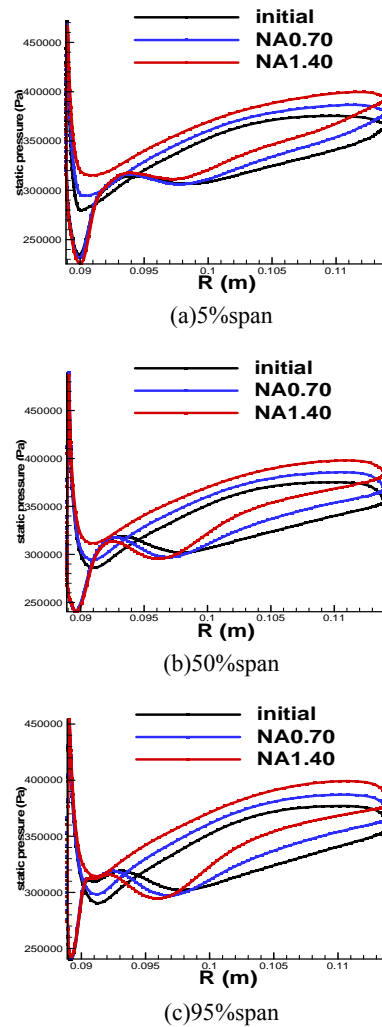


Fig. 12. Blade loading of the diffuser

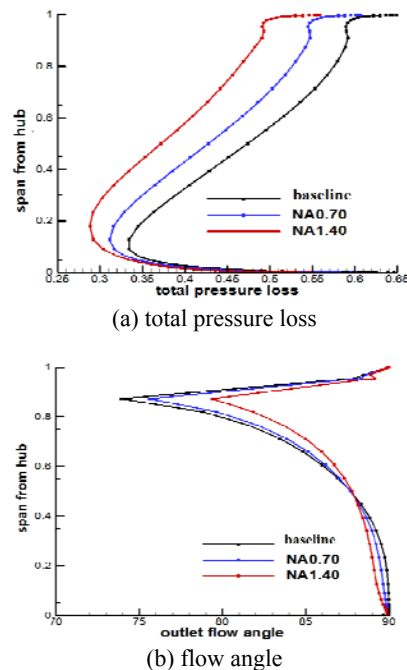


Fig. 13. Aerodynamic parameter at diffuser outlet

than that of the hub, which is caused by the corner separation gathering near the shroud. The total pressure loss decreased significantly in whole spanwise range for those two diffusers with non-axisymmetric endwall profiling. Benefit from the reduction in the corner separation size and corner separation intensity, the reduction of the flow loss is more notable near the shroud.

From the distribution of the flow angle at diffuser outlet in Fig. 13b, it can be seen that the flow overturning strength is reduced from 40% span to the shroud by the optimized endwall profiling, and the overturning is also weakened below 40% span, thus the distribution of the flow angle is more uniform, which is good for the flow field. Furthermore, the improvement of flow field by the non-axisymmetric endwall profiling extends to the whole span due to the small aspect ratio of the diffuser vane.

### 4.3 Comparison Between Non-axisymmetric Endwall and Tandem Cascade

Figure 14 gives the comparison of flow field between non-axisymmetric endwall of NA1.40 and tandem cascade at 70% span under the design condition. The flow separation on suction side of the diffuser is all effectively suppressed through these two flow control approaches. For non-axisymmetric endwall of NA1.40, this task is fulfilled by the upward convexity structure of the suction surface, where the low-energy fluid which easily inducing the flow separation can be accelerated. From the streamline of the tandem cascade, the visible flow separation appears near the trailing edge of the suction side of the front vane. The flow field improvement by the tandem cascade mainly takes effect on the rear vane, and the radial gap between the front vane and the rear vane is the key factor to restrain the flow separation. The high-velocity flow from pressure side of the front vane goes through this gap, then arrives at the suction side of rear vane. Similar to the boundary layer suction device, the low-energy fluid of the rear vane row is blown off, and the flow separation can be depressed effectively, the original large-scale corner separation is split into two smaller vortices, thus the less flow loss and better performance of the diffuser can be achieved.

It needs to point out that the supersonic flow near the leading edge of the tandem cascade gets an extra acceleration, followed by the decreased static pressure in that region, while this phenomenon does not happen for the diffuser with non-axisymmetric endwall of NA1.40. For the subsonic flow region in the diffuser passage, static pressure distribution of the tandem cascade is more uniform, which means the smaller blade loading in the tandem cascade diffuser. When the non-axisymmetric endwall is performed, the pressure gradient is relatively higher than that it has for the tandem cascade diffuser.

The limiting streamlines with radial velocity contour on the suction surface of the diffuser are displayed in Fig. 15a. The flow separation can be

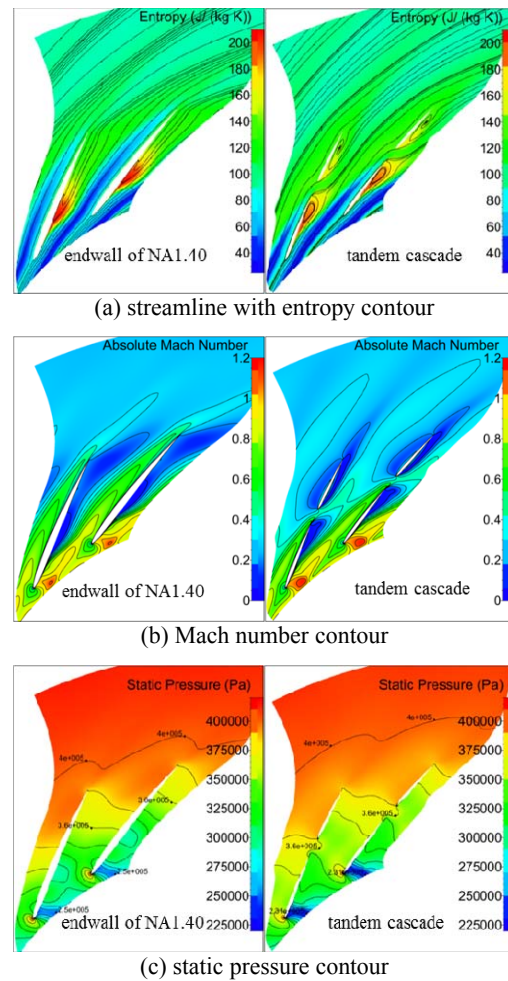
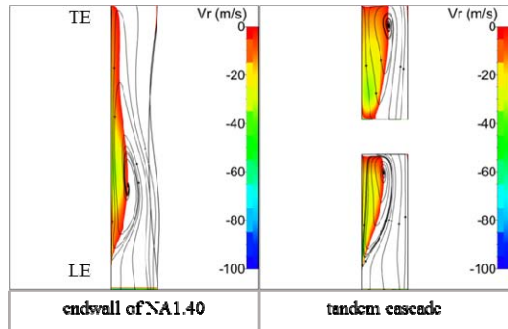


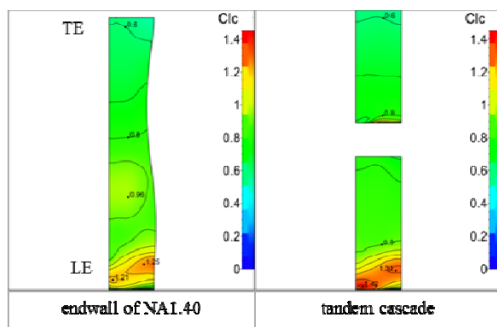
**Fig. 14. Flow field of different structures at 70% span**

inhibited to a certain extent by these two approaches. The flow separation range is decreased by profiled endwall of NA1.40. The original large-scale flow separation zone is transformed into two smaller vortices by the tandem cascade, and the corresponding flow separation extent is still greater than the diffuser with non-axisymmetric endwall profiling. Figures 15b and 15c respectively show the total pressure loss coefficient distribution on two sides of the vane, where the rear row location of the tandem cascade is in line with the rear part of diffuser with non-axisymmetric endwall of NA1.40, and the loss distribution also presents a consistent trend in these two zones. However, the total pressure loss at the front row inlet of the tandem cascade is obviously higher than that of NA1.40 at the same position. According to the Mach number distribution, it can be found that the high flow loss is derived from the supersonic region near the leading edge of the diffuser. On the pressure surface, the overall loss of the front row of the tandem cascade is significantly lower than that it has in the front part of the diffuser in NA1.40. For the subsonic flow, the tandem cascade performs the capacity for work through two rows, the blade loading can be effectively reduced, the increment of the thickness of the boundary layer can be efficiently controlled, and the flow separation can

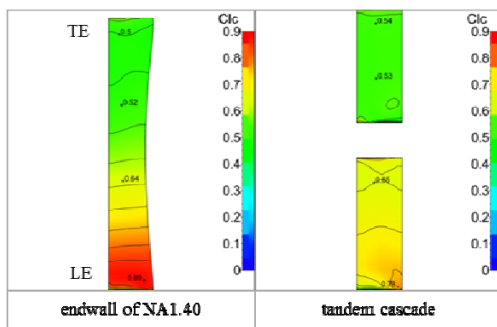
be suppressed. But once the supersonic flow occurs in the diffuser, it turns out to be out of control in the tandem cascade diffuser, and the increasing flow loss exposes this disadvantage clearly.



(a) limit streamline with Vr contour on suction surface



(b) total pressure loss contour on suction surface



(c) total pressure loss contour on pressure surface

**Fig. 15. Flow field of different structures on the diffuser vane**

#### 4.4 Flow Field Under Off-design Condition

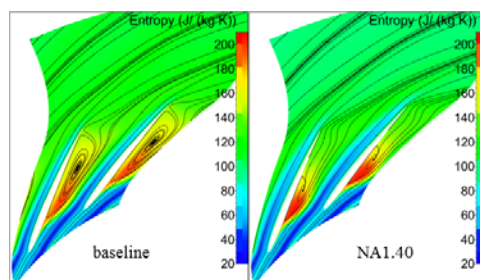
In order to explore the potential of the non-axisymmetric endwall, the flow field of the diffuser with non-axisymmetric endwall of NA1.40 is also investigated under the off-design condition, and compared with the baseline diffuser. The performance parameters of the centrifugal compressor stage is depicted in Table 3, with minimum flow rate of 1.047kg/s. Compared with the baseline diffuser, the diffuser with non-axisymmetric endwall still displays better performance under off-design condition, but the efficiency gain falls to 3.21%.

Figure 16 presents entropy and Mach number distribution at 70% span of the vane for the baseline diffuser and diffuser with non-axisymmetric endwall of NA1.40. Apparent flow separation

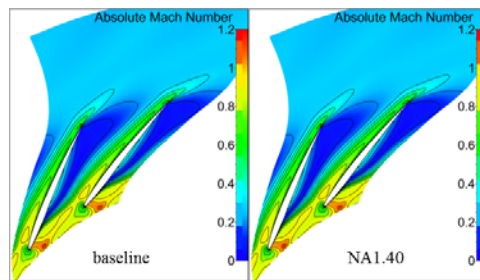
appears in the baseline diffuser, which nearly occupies the whole passage in the rear part of the vane. Non-axisymmetric endwall of NA1.40 has a certain acceleration effect on the flow, a slight flow separation still occurs in the middle of the suction side. Under the off-design condition, the ability of the non-axisymmetric endwall to suppress the flow separation becomes weaker, inevitably lower the effectiveness of the performance improvement as compared with the design condition.

**Table 3 Performance parameters under off-design condition**

	$\eta$	$\Delta\eta$ (%)	$C_{LC}$	$\Delta C_{LC}$ (%)
baseline	0.7563	0	0.4409	0
NA1.40	0.7806	3.21	0.3696	-16.16



(a) streamline with entropy

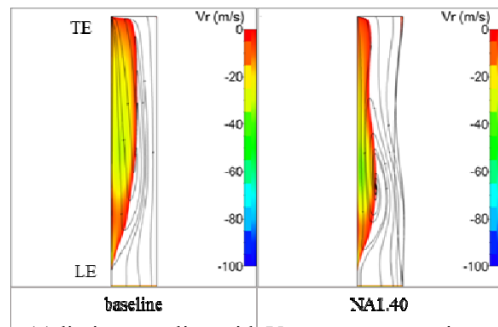


(b) Mach number

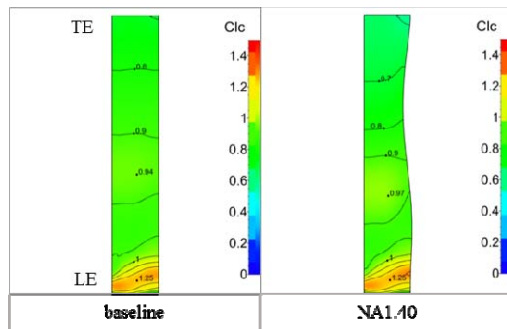
**Fig. 16. Flow field in the diffuser at 70% span under off-design condition**

Figure 17 shows the flow field on the diffuser vane under off-design condition. From Fig. 17a, the limit streamline on the suction surface reveals the massive flow separation occurred in the baseline diffuser. For the case of NA1.40, the vortex is pushed towards the shroud with less effect on the flow. But the magnitude of the maximum velocity in the backflow zone becomes larger than that it has for the baseline diffuser, the energy of the separated fluid congregates into the vortex core further. The total pressure loss distribution on the diffuser vanes are shown in Figs. 17b and 17c, and a similar variation can be observed in the rear part of the vane. When the non-axisymmetric endwall is adopted, the overall total pressure loss on the suction side and the pressure side are reduced by 12.50% and 15.38%, respectively. The reduction of total pressure loss remains on the whole pressure surface for the case of NA1.40, however, local rise of the total pressure loss appears in the front part of suction surface, the total pressure loss even increases by 3.19% in the

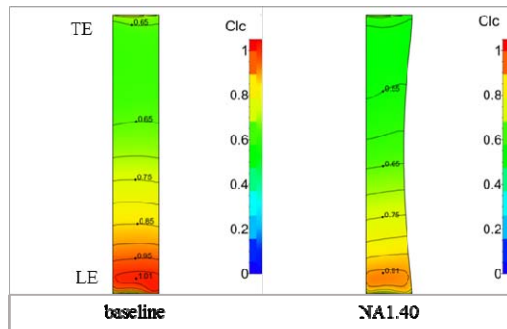
region with maximum backflow velocity, partially balancing out the benefit for the performance improvement of the non-axisymmetric endwall.



(a) limit streamline with Vr contour on suction surface



(b) total pressure loss contour on suction surface



(c) total pressure loss contour on pressure surface

**Fig. 17. Flow field on the diffuser vane under off-design condition**

Under the condition of smaller flow rate, it turns out to be difficult to control the local converging flow within the flow separation zone for the non-axisymmetric endwall, the flow field improvement effectiveness of the non-axisymmetric endwall profiling decreases correspondingly. Near the shroud of the diffuser, the backflow with high velocity makes the mass flow rate decrease, which is easier to induce the stall, thereby the operating flow range is reduced when the non-axisymmetric endwall profiling is performed for the diffuser.

## 5. CONCLUSIONS

In this paper, the non-axisymmetric endwall optimization was conducted for the diffuser of a transonic centrifugal compressor under design condition, with the objective to maximize the isentropic efficiency of the compressor stage.

Numerical simulations were performed for the compressor stage with baseline and profiled endwalls, the flow field and performance characteristics were analyzed, and the tandem cascade diffuser was also investigated for comparison. Main conclusions can be drawn as follows:

1) The ability of tandem cascade diffuser to improve the compressor performance under design condition is between non-axisymmetric endwall of NA0.70 and NA1.40. Compared with the tandem cascade diffuser, non-axisymmetric endwall profiling is an effective way to significantly reduce the flow loss in the diffuser. The total pressure loss of the diffuser decreases by 9.31% and 20.29% for NA0.70 and NA1.40 respectively, and the responding isentropic efficiency gain is 1.68% and 3.63%. The purpose of improving the efficiency in the steady operation flow range, can be achieved by optimized non-axisymmetric endwall profiling. However, the benefit of the non-axisymmetric endwall profiling for the performance is partially balanced out under off-design condition, because of the reduced acceleration effect on the low-energy fluid. The backflow with high velocity gathering near the diffuser shroud, makes the mass flow rate decrease, then reduces the stable operating flow range. The operation range of the compressor stage decreases by 11.50% for the case of NA0.70, while the reduction of NA1.40 reaches up to 22.12%.

2) Under the design condition, serious corner separation occurs on the suction side of the baseline diffuser, resulting in a sharp rise of the flow loss. The optimized endwalls profiling are mainly characterized by upward convexity on the whole pressure side and rear part of the suction side, while a small locally downward concave is formed in the front part of suction side. The upward convexity structure of the profiled endwall can accelerate the low-energy flow of the separated vortex, thus the corner separation is effectively suppressed. The corresponding high vorticity within the flow separation zone is reduced, which delays the formation and development of the flow separation. The smaller lateral pressure difference in the rear part of the diffuser passage, is another reason for suppression of the flow separation.

3) When the non-axisymmetric endwall profiling is performed, the diffuser becomes more fore-loaded, the overall blade loading is not affected, and the pressure ratio of the compressor stage is improved as well. Owing to the small aspect ratio of the diffuser vane, the influence of the non-axisymmetric endwall profiling extends from the hub to the shroud of the diffuser. Thus, the more uniform distribution of the flow angle and lower total pressure loss at diffuser outlet are both achieved simultaneously.

## ACKNOWLEDGEMENTS

The author(s) disclosed receipt of the following financial support for the research, authorship, and/or publication of this article: This work was

supported by National Natural Science Foundation of China (No. 51576163 and No.51876176), MIT and the Fundamental Research Funds for the Central Universities (No. 3102018gxc003).

## REFERENCES

- Chu, W., X. Li and Y. Wu (2016). Reduction of end wall loss in axial compressor by using non-axisymmetric profiled endwall: A new design approach based on end wall velocity modification. *Aerospace Science & Technology* 55, 76-91.
- Demeulenaere, A., A. Purwanto, A. Ligout *et al.* (2005 June). Design and optimization of an industrial pump: application of genetic algorithms and neural network. In *ASME Fluids Engineering Division Summer Meeting*, Houston, TX, USA, FEDSM2005-77487
- Ferrara, G., L. Ferrari and C. P. Mengoni (2002, June). Experimental investigation and characterization of the rotating stall in a high pressure centrifugal compressor: Part I: influence of diffuser geometry on stall inception. In *Proceeding of ASME TURBO EXPO 2002*, Amsterdam, Netherlands, GT-2002-30389.
- Ferrara, G., L. Ferrari and C. P. Mengoni (2002, June). Experimental investigation and characterization of the rotating stall in a high pressure centrifugal compressor: part II: influence of diffuser geometry on stage performance. In *Proceeding of ASME TURBO EXPO 2002*, Amsterdam, Netherlands, GT-2002-30390.
- Gao, L. M., G. Xi and L. Zhou (2005). Experimental and computational investigation of flows in a vaned diffuser under stage environment. *ACTA Mechanical SINICA* 37(1), 110-119.
- Guo, Z. D., L. M. Song and H. Sun (2016). Aerodynamic optimization of a 3D parameterized turbine vane with non-axisymmetric endwall. *Journal of Engineering Thermophysics* 37(2), 285-289.
- Harvey, N. W. (2008, June). Some effects of non-axisymmetric end wall profiling on axial flow compressor aerodynamics: Part I — linear cascade investigation. In *Proceeding of ASME TURBO EXPO 2008*, Berlin, Germany, GT-2008-50990.
- Harvey, N. W. and T. P. Offord (2008, June). Some effects of non-axisymmetric end wall profiling on axial flow compressor aerodynamics: Part II — multi-stage HPC CFD study. In *Proceeding of ASME TURBO EXPO 2008*, Berlin, Germany, GT-2008-50991.
- Hoeger, M., P. Cardamone and L. Fottner (2002, June). Influence of endwall contouring on the transonic flow in a compressor blade. In *Proceeding of ASME TURBO EXPO 2002*, Amsterdam, Netherlands, GT-2002-30440.
- Li, G. J., X. Y. Ma and J. Li (2005). Non-axisymmetric turbine end wall profiling and numerical investigation of its effect on the turbine cascade loss. *Journal of Xi'an Jiaotong University* 39(11), 1169-1172.
- Liu, B., J. W. Guan and Y. Y. Chen (2008). Numerical investigation for effect of non-axisymmetric endwall profiling on secondary flow in turbine cascade. *Journal of Propulsion Technology* 29(3), 355-359.
- Morris, A. W. H. and R. G. Hoare (1975, June). Secondary loss measurements in a cascade of turbine blades with meridional wall profiling. *ASME 75-WA*, GT-1975-13.
- Mukkavilli, P., G. R. Raju and A. Dasgupta (2002, June). Flow Studies on a Centrifugal Compressor Stage With Low Solidity Diffuser Vanes. In *Proceeding of ASME TURBO EXPO 2002*, Amsterdam, Netherlands, GT-2002-30386.
- Nage, M. G. and R. D. Baier (2005). Experimentally verified numerical optimization of a 3D-parametrised turbine vane with non-axisymmetric end walls. *Journal of Turbomachinery* 127(2), 380-387.
- Poehler, T., J. Niewoehner and P. Jeschke (2015). Investigation of non-axisymmetric endwall contouring and three-dimensional airfoil design in a 1.5-stage axial turbine—Part I: design and novel numerical analysis method. *Journal of Turbomachinery* 137 (8), 081009.
- Poehler, T., J. Niewoehner and P. Jeschke (2015). Investigation of non-axisymmetric endwall contouring and three-dimensional airfoil design in a 1.5 stage axial turbine — Part II: experimental validation. *Journal of Turbomachinery* 137(8), 081010.
- Rose, M. G. (1994, June). Non-axisymmetric endwall profiling in the HP NGVs of an axial flow gas turbine. In *International Gas Turbine and Aeroengine Congress and Exposition*, Hague, Netherlands, 94-GT-294.
- Wu, J. C., X. G. Lu and J. Q. Zhu (2011). Secondary flow analysis for non-axisymmetric endwall on the high-load compressor cascade. *Journal of Aerospace Power* 26(6), 1362-08.
- Wang, Y., X. G. Lu and S. F. Zhao (2011). Effects of diffuser blade geometry at leading edge on a highly-loaded centrifugal compressor. *Journal of Propulsion Technology* 32(2), 175-181.
- Xi, G., L. Zhou and H. P. Ding (2006). Numerical and experimental study of the effects of the stagger angles of vane diffuser on the performance of centrifugal compressors. *Journal of Engineering Thermophysics* 27(1), 61-64.
- Zhang, C. L., Q. H. Deng and Z. P. Feng (2009). Aerodynamic optimization design of vaned

- diffuser for centrifugal compressor under stage environment. *Journal of Xi ' an Jiaotong University* 43(11), 32-36.
- Zhang, P., B. Liu and Z. Y. Cao (2014). Optimization design for counter-rotating compressor with non-axisymmetric endwall contouring. *Journal of Aerospace Power* 29(11), 2570-2578.
- Zhao, X. L. and W. Wang (1997). Numerical studies of low-solidity tandem cascade diffusers. *Journal of Engineering Thermophysics* 18(2), 186-189.
- Zhao, S. F., J. F. Luo and X. G. Lu (2009). Exploring the aerodynamic feasibility of substituting aspirated cascade for tandem cascade. *Journal of Engineering Thermophysics* 30(7), 1109-1112.